Received: 13 October 2020 | Revised: 8 February 2021 | Accepted: 1 March 2021

DOI: 10.1002/er.6676

RESEARCH ARTICLE

INTERNATIONAL JOURNAL OF ENERGY RESEARCH WILEY

A novel resource allocation model based on the modularity concept for resiliency enhancement in electric distribution networks

Saeed Mousavizadeh[1] | **Arman Alahyari**[2] | **Tohid Ghanizadeh Bolandi**[3] | **Mahmoud-Reza Haghifam**[1] | **Pierluigi Siano**[4]

[1]Faculty of Electrical and Computer Engineering, Tarbiat Modares University, Tehran, Iran

[2]Center for Energy Systems, Skolkovo Institute of Science and Technology (Skoltech), Moscow, Russia

[3]Faculty of Electrical and Computer Engineering, Urmia University, Urmia, Iran

[4]Department of Management & Innovation Systems, University of Salerno, Fisciano, Italy

Correspondence
Tohid Ghanizadeh Bolandi, Faculty of Electrical and Computer Engineering, Urmia University, Urmia, PO Box 5756151818, Iran.
Email: t.ghanizadehbolandi@urmia.ac.ir

[Correction added on 6 April 2021, after first online publication: the name of the first author has been corrected.]

Summary

Paying attention to the modularity feature of electric distribution systems improves their performance against severe events and makes an outstanding opportunity for resiliency enhancement. In this paper, a novel framework based on the modularity concept is proposed in which, by deploying smart grid technologies and forming efficient modules, effective and robust energy in distribution systems is provided. Optimal placement of distributed generation (DG) resources, load control options, switching devices, and tie lines are simultaneously incorporated in the proposed linear allocation model. To consider electrical and topological characteristics in the independent functioning of the formed modules, a path-based method is employed. The effectiveness and computability of the proposed algorithm are examined by performing several simulations on two modified 37-bus and 84-bus test systems. The results demonstrate that the developed modular structure, by subdividing the system into several independent parts, creates more flexibility for the recovery process and facilitates the self-healing capabilities.

KEYWORDS

distribution network, linear programming, microgrids, modularity, resiliency

1 | INTRODUCTION

The occurrence of natural disasters in last decades, their destructive effects on the electric power system, and consequently, the resulted disruptions of social and economic affairs have highlighted the necessity of resiliency analysis.[1,2] Resiliency concept investigates the ability of a system to tolerate high impact and low probable (HILP) events and has been considered in many studies.[3,4] The main objective of these studies is to ensure lowest interruptions and restores the system to a normal condition as soon as possible.[5,6] In such circumstances, due to the severity of events and their related uncertainties, as well as the specific structure and characteristics of distribution networks, limited corrective actions and emergency plans can be implemented by the electric utilities.[7] In order to achieve a resilient distribution network against HILP events, the planning and operation activities of the distribution network should be upgraded prior, during, and after the disasters.[8] In this regards, optimal deployment of smart grid technologies and forming the efficient microgrids is of paramount importance.[9]

Several studies have researched the potential measures and the possible remedial actions for preventing the extensive outages and deteriorating the impacts of such disasters in distribution networks. According to the

time domain, these measures can be divided into two categories. The first category considers short-term horizons and focuses on the scheduling of operational activities. Pre-event allocation of available resources to enhance the system withstanding[10-16] and provision of post-event restoration strategies like microgrid (MG) formation[17-19] are the main contributions of these research studies. On the other hand, the second category addresses the system resiliency enhancement from the planning point of view by optimally investing and modernizing the network,[20,21] hardening the infrastructures,[22] optimal resource allocation,[23] fast and effective restoration planning,[24] and considering the repair crew.[25] The scope of the proposed method in this paper falls into second category. Therefore, the literature review focuses mainly on this category.

Although the topic of the resilient operation of distribution networks has been widely studied in recent papers, network expansion and investment planning issues from the resiliency point of view are at their early stages. Resilience-based distribution network planning methods should be implemented before the occurrence of disaster to minimize its destructive effect. Previous research on investment models can also be classified into two groups. In the first group, for modeling the event intensity and examining its impacts on system functioning, probabilistic models and stochastic programming frameworks are utilized.[26-30] In these methods, fragility curves are generally applied to calculate the failure probability of the system components in case of disasters. Therefore, in these approaches, it is necessary to predict the severity of the event and its impacts on equipment performances. Due to the imprecise prediction of severity of such catastrophes (because of their extremely volatile nature), and the lack of adequate information about the equipment fatigue and operation conditions in distribution networks, extracting the fragility curves and applying the calculated failure probabilities in long-term studies, like network expansion problems, are not effective. Therefore, such methods do not provide solid foundations for investment models.

In the second category of investment studies,[31-35] decision-making about the improvement schemes is carried out by utilizing robust optimization-based frameworks and applying the defender-attacker models. In these approaches, the system defender prepares for the worst-case contingencies while considering different hardening budgets and applying various attack levels (severity of the event). These models utilize a sequential game according to which, in the first stage, defender deploys an investment plan and in the second stage, attacker disrupts the system aiming at the maximum damage by finding the worst cases. These papers mostly focus on lines hardening[31,32] or network expansions in transmission systems.[33] In References 31, 32 it is assumed that by implementing reinforcements on system components, the hardened lines can survive the disasters. In Reference 34 an optimal hardening plan for improvement of the resilience of integrated electricity and natural gas distribution network against natural disasters is proposed. In Reference 35 an optimal strategy for resilience enhancement in distribution networks is introduced based on energy storage system deployment and line hardening. The proposed approach is formulated as a multistage multizone defender-attacker-defender model to consider the random contingencies. Since in these methods, only the intensity of the event is considered; it is not feasible to make a distinction between the events with the same severity. Therefore, the robust functioning of the reinforced components against all these kind of events is not valid. Besides, since in these approaches for each attack level a reinforcement plan is designed, the system will be fragile and vulnerable against higher intensities of events. These methods, indeed, mainly focus on improving the system performance from a robustness perspective instead of focusing on resiliency.

Resource allocation is one of the resilience-based distribution network planning approaches which should be optimally implemented before the occurrence of HILP events to proactivate the network recovery in the fastest time possible. In Reference 23 a disaster response–based model is presented to support the emergency loads during HILP events by maximizing the operational capacity. In Reference 36 a resilience-based prehurricane resource allocation model is proposed in distribution network by allocating the diesel generators and batteries to serve the critical loads. Optimal allocation of photovoltaic generation and battery storage is proposed in Reference 37, for resilience enhancement in distribution networks based on a multiobjective optimization model. In Reference 38, a resource allocation model including the distributed generations and demand responsive loads is proposed using microgrid formation approach in postevent to improve the resiliency of distribution networks. In Reference 39, a resilient microgrid formation approach is introduced to enable the critical load restoration considering master-slave-based DGs and topology reconfiguration. In the mentioned methods for resource allocation, the development of switching capabilities, the placement of tie lines, allocation of generation resources, and implementing the demand side controlling options are not simultaneously considered in the proposed models. Additionally, the resource allocation methods should be optimally implemented to form the effective microgrids in postdisaster to impressively improve the distribution network resiliency.

Development of smart grid facilities empowers the system to form the self-provided modules, which can be employed independently or collaboratively as an MG after the event. Modularizing the structure prepares the system for severe conditions and improves the resiliency, regardless of the intensity or the type of disasters. However, achieving an appropriate level of modularity in distribution networks requires the optimal expansion of smart grid technologies. Recent research in this field lacks a comprehensive framework for improving system functioning from the modularity perspectives.

In this paper, based on the modularity concept, a linear budget allocation model is presented for achieving an effective investment in distribution network facilities to improve the resiliency of distribution networks. The proposed framework, by enhancing the ability of MGs formation and applying appropriate switching, guarantees the provision of electrical loads in efficient modules during the severe contingencies. Optimal placement and allocation of DG resources, switching devices (sectionalizers and tie lines), as well as load control capabilities, are the main purpose of this resource allocation problem. To model the topological characteristics and structural limitations of the network and also for determining the coverage areas of the formed modules, a linear path-based method is utilized. Note that, the proposed approach is a systematic one which is not focusing on the type of an event or a cause or details such as the fragility of poles and lines in the network. Rather, the proposed novel method seeks to investigate the impact of modularity on the resiliency of a power network in different conditions. Besides, the proposed approach aims at identifying an investment plan and, in this regard, does not focus on the short-term operations. Note that in this study, we assume that the DGs have nonintermittent production[8]; however, the proposed methodology can be further expanded in the next stage of research to include the DGs with uncertain production as well through the related uncertainty modeling such as those introduced in References 40-44 In conclusion, the most important contributions of the proposed method can be categorized as follows:

- Introducing a novel conceptual framework to improve the resiliency of distribution networks based on the modularity idea to form the effective microgrids.
- Presenting a new linear budget allocation model for achieving the desired level of self-healing options through the optimal placement of smart grid facilities.
- Simultaneous and optimal incorporating of the DG resources, load control options, switching devices, and tie lines in the proposed resource allocation model.
- Providing a fitting defensive strategy for resiliency enhancement, this is more coordinated with the development of MG technology and decentralized power supplies.

To confirm the superiority and novelty of the proposed resilient resource allocation approach, its performance is compared with some existing research findings which are recently published in the field of resiliency enhancement in distribution networks. In this regards, the comparison between the proposed method with other approaches presented in the literatures is reported in Table 1 in eight aspects. These aspects are the resilient resource allocation based on modularity concept, optimal resource allocation including demand curtailment options, DG resources or energy storage systems (ESS),

TABLE 1 Proposed method vs pervious published schemes

Comparison aspect	[25]-2020	[35]-2020	[36]-2017	[37]-2017	[38]-2017	[39]-2017	[45]-2019	[46]-2021	Proposed method
Resilient resource allocation based on modularity concept	×	×	×	×	×	×	×	×	✓
Optimal allocation of the demand curtailment options (load control options)	×	×	×	×	✓	×	×	×	✓
Optimal allocation of the DG/ESS resources	×	✓	✓	✓	✓	✓	✓	✓	✓
Optimal placement of the switching devices (sectionalizers)	×	×	×	×	×	×	×	✓	✓
Optimal placement of the tie lines	×	×	×	×	×	×	✓	×	✓
Presenting a linear budget allocation model	✓	✓	×	✓	✓	×	✓	✓	✓
Forming the optimal arrangement of efficient and independent microgrids for maximum critical load restoration	✓	×	×	×	✓	✓	✓	✓	✓
Introducing a novel resiliency index	×	✓	✓	×	×	×	✓	✓	✓

switching devices and tie lines, presenting a linear budget allocation model, forming the optimal arrangement of efficient and independent microgrids for maximum critical load restoration, and introducing a novel resiliency index. As can be seen, the proposed method performs better than the existing methods in modeling of all mentioned aspects. Additionally, to the best knowledge of the authors, no attempts have been reported on presenting a comprehensive model for implementing the optimal resource allocation from the modularity perspectives to improve the resilience of distribution network. The proposed approach also leads to the achievement of an effective investment plan in distribution network facilities. Consequently, the proposed model has significant advantages over existing methods.

The remainder of the paper is as follows. In section 2, the background of the proposed approach is discussed. The mathematical formulation of the investment problem is described in section 3. In section 4, the effectiveness of the proposed algorithm is examined by performing several simulations. Finally, section 5 concludes the study.

2 | ENABLING MODULARITY

Building a modular structure and decomposing the system into several self-provided modules facilitate isolation of the damaged parts in case of contingency and accelerate load restoration in intact sections after extensive outages.[47] The efficiency of a module is defined based on the value of involved consumptions in that module and its dependency level on equipment. These two factors have conflicts with each other. In other word, efficient modules supply more loads with a lower number of components in a power system. Consequently, in a well-modularized system, after severe disasters and failing of multiple elements, feeding the electrical loads will be easier. Furthermore, after a catastrophe, depending on the locations of the faults, each module can supply independently its loads as an MG or the undamaged modules can bond together and provide the loads through forming a larger MG.

For example, as shown in Figure 1, considering the capacity of DGs and switching options, after a severe event, one self-provided module (*M1*) can be formed, only if all of the required elements for creating that module will not be in a failure state. After installation of the sectionalizer *S3*, *M1* is decomposed into smaller parts, and two modules (*M2* and *M3*) can be formed. As *M1* includes a higher number of elements, it is more susceptible to damage in case of an event, and, consequently, it suffers from a high vulnerability situation if compared to *M2* and *M3*. As a result, by adding the mentioned switch, the system modularity is enriched, and the located consumers in *M2* and *M3* experience a higher resistance and recoverability than the former case. In other words, load provision in the latter case will be more resilient.

3 | PROBLEM FORMULATIONS

In this paper, we consider the simultaneous allocation of the demand curtailment options, DG resources, tile lines, and sectionalizers for the peak load condition. Other measures like hardening of the power lines will be considered in our future works. Besides, since in severe weather circumstances, operation of the renewable energy resources is not conceivable, and due to their poor capability in stabilizing the voltage and frequency of the modules, only the controllable DGs such as diesel generations are included in the model. Renewable energies can be accommodated by reformulating the planning problem and creating a two-stage decision framework. As

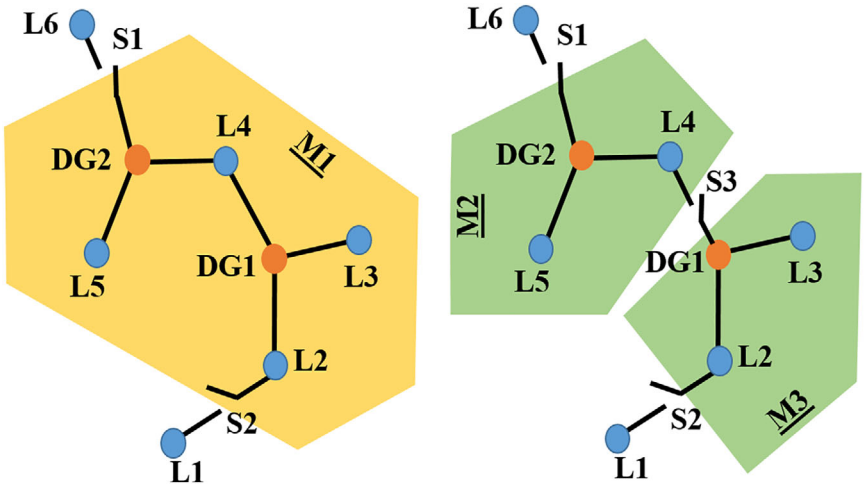

FIGURE 1 System modularization [Colour figure can be viewed at wileyonlinelibrary.com]

mentioned in Reference 48, minimizing a linear function with linear constraints is often algorithmically simpler and more efficient than its nonlinear counterpart. Therefore, we perform the linearization of constraints if needed to derive an MILP problem that can be solved effectively by a well-known solver such as CPLEX.

3.1 | Topological constraints

At first, considering all the buses and lines (including candidate tie lines), the graph of the network is extracted. For technical issues, the connection of at least one DG to each formed module is necessary. This DG is called master unit and its corresponding node is recognized as the root node of that module.

3.1.1 | Node belonging constraints

According to Equation (1), a node can be included in only one of the modules or none of them. If the variable $\alpha_{i,k}$ is equal to one, node i belongs to module k, and the kth member of the set N_{DG} is selected as the master unit. If the selected unit is also a member which belongs to set of candidate DGs in N_{Ca_DG}, it means that the unit is considered for installation.

$$\sum_{k=1}^{Num_{Mds}^{Max}} \alpha_{i,k} \le 1 \quad \forall i \in N \tag{1}$$

Besides, as given in Equation (2), for connecting a node to a module, at least one of its parent nodes should be involved in that module. Parents of a node are the first nodes in the paths between that node and the root. For example, in Figure 2, nodes m, n, p, and q are the parents of node i for reaching the root node k.

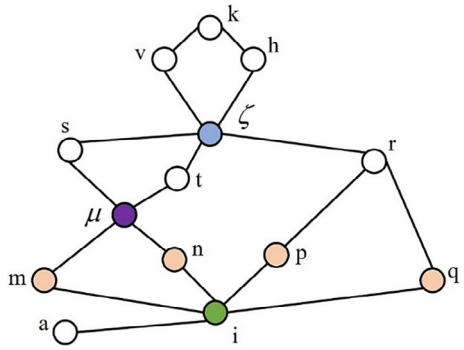

FIGURE 2 Sample graph of a network [Colour figure can be viewed at wileyonlinelibrary.com]

$$\alpha_{i,k} \le \sum_{\forall j \in \xi_{i,k}} \alpha_{j,k} \quad \forall i \in N, \forall j \in \xi_{i,k}, \forall k \in K \tag{2}$$

3.1.2 | Interconnected and radial structure

In order to satisfy the constraints of connectivity and radial configuration of each module, a path-based method is employed for formulating them. For each node, the entire paths between that node (as a start point) and a root node (as an end) are explored. Then, intersections of the extracted paths are analyzed, and finding a common node (excluding start point) among them is investigated. At the next step, first, constraints of connectivity and radial configuration are guaranteed between that start node and the first founded common node, and then these constraints are applied to the existing paths between that common node and the root node. For example, as shown in Figure 2, first the mentioned constraints are checked for the paths between nodes i and ζ, then the paths between the common node ζ and the root node k are taken into account. The method presented in Reference 49 is employed here for finding the common node.

Based on the previous comments, Equations (3) and (4) are applied to ensure the connectivity constraint between hypothetical node i and its common node (node ζ). Equation (3) states that if node i is included in module k, then the existed common node on the corresponding paths should belong to that module. Equation (4) ensures that one of the existing paths should be in an active state in case of connection to the corresponding module.

$$\alpha_{i,k} \le \alpha_{\zeta,k} \quad \forall k \in K \tag{3}$$

$$\sum_{x=1}^{NumPath_{i-z}} \mathrm{Path}_{i-\zeta}^{x} \ge \alpha_{i,k} \quad \forall k \in K, \forall x \in \ Allpath_{i-z} \tag{4}$$

Additionally, according to Equation (5), the status of each path is dependent on the states of the involved lines. Note that, β_ℓ is a binary variable that indicates the operation mode of a line. The set of the equations in (6) is utilized for linearizing the Equation (5).

$$\mathrm{Path}_{i-\zeta}^{x} = \prod_{\ell \in \Lambda_{i-\zeta}^{x}} \beta_\ell \quad \forall x \in \ Allpath_{i-z} \tag{5}$$

$$\begin{cases} \mathrm{Path}_{i-\zeta}^{x} \le \beta_\ell \quad \forall x \in \ Allpath_{i-z}, \forall \ell \in \Lambda_{i-\zeta}^{x} \\ \mathrm{Path}_{i-\zeta}^{x} \ge \sum_{\forall \ell \in \Lambda_{i-\zeta}^{x}} \beta_\ell - \left(NumLine_{i-\zeta}^{x} - 1 \right) \quad \forall x \in \ Allpath_{i-z} \end{cases} \tag{6}$$

Moreover, if there are several paths between two nodes (eg, nodes μ and i) achieving a radial configuration should be ensured as well. Equation (7) states that for avoiding loops, at least one of the variables indicating the statues of the involved lines should be set to zero.

$$\sum_{\forall \ell \in \Lambda^{z}_{i-\mu}} \beta_{\ell} + \sum_{\forall \ell' \in \Lambda^{z'}_{i-\mu}} \beta_{\ell'} \leq \left(NumLine^{z}_{i-\mu} + NumLine^{z'}_{i-\mu} - 1 \right), \quad \forall z \in \ Allpath_{i-m} \tag{7}$$

It is worth to notice that the structure of modules is assumed to be radial to decrease the complexity and better certify the merit of the approach and to open an avenue toward the future similar research. Note that, the proposed approach can be modified to consider the meshed structure as well which would be considered in the future works.

3.1.3 | Boundary constraints

According to (8), the variable β_{ℓ} should be set to zero, if two sides of a line belong to the same module. Symbol $\odot$ represents the logical XNOR operation. By defining auxiliary binary variables $\chi_{\ell,k}$ and $\chi'_{\ell,k}$, the Equation (8) could be linearized using the presented set of equations in (9).

$$\beta_{\ell} < \alpha_{i,k} \odot \alpha_{j,k} \quad \forall \ell \in \Lambda, \forall i,j \in \Psi_{\ell}, \forall k \in K \tag{8}$$

$$\begin{cases} \beta_{\ell} < \chi_{\ell,k} + \chi'_{\ell,k} \quad \forall \ell \in \Lambda, \forall k \in K \\ \chi'_{\ell,k} \leq 1 - \alpha_{i,k}\ , \ \chi_{\ell,k} \leq \alpha_{i,k} \quad \forall i,j \in \Psi_{\ell}, \forall \ell \in \Lambda, \forall k \in K \\ \chi'_{\ell,k} \leq 1 - \alpha_{j,k},\ \chi_{\ell,k} \leq \alpha_{j,k} \quad \forall i,j \in \Psi_{\ell}, \forall \ell \in \Lambda, \forall k \in K \\ \chi'_{\ell,k} \geq 1 - \alpha_{i,k} - \alpha_{j,k}\ , \chi_{\ell,k} \geq \alpha_{i,k} + \alpha_{j,k} - 1 \quad \forall i,j \in \Psi_{\ell}, \forall \ell \in \Lambda, \forall k \in K \end{cases} \tag{9}$$

3.1.4 | Switching constraints

Equations (10) and (11) ensure the closed mode for the lines which do not include switching option.

$$Sec_{\ell} = 1 \quad \forall \ell \in \Lambda^{ST} \tag{10}$$

$$\beta_{\ell} \geq (1 - Sec_{\ell}) \quad \forall \ell \in \Lambda \tag{11}$$

3.2 | Electrical constraints

3.2.1 | Demand consumptions

Equations (12) to (14) are utilized to formulate the amount of active and reactive power consumptions considering curtailment capabilities. In Equation (14), $P^{LC,Im}_{i}$ is a decision variable and is described in the budget constraint section.

$$P^{L}_{i,k} = \alpha_{i,k} \times \mathrm{P}^{Load}_{i} - P^{LC,Im}_{i,k} \quad \forall k \in K, \quad \forall i \in N \tag{12}$$

$$Q^{L}_{i,k} = \alpha_{i,k} \times Q^{Load}_{i} - \tan(\varphi_i) \times P^{LC,Im}_{i,k} \quad \forall k \in K, \quad \forall i \in N \tag{13}$$

$$P^{LC,Im}_{i,k} \leq \alpha_{i,k} \times \mathrm{P}^{Load}_{i} \quad \forall k \in K, \quad \forall i \in \overline{N} \subset N \tag{14}$$

3.2.2 | DG constraints

To model the active and reactive power limits for all the existed and candidate DGs, Equations (15) and (16) are applied. In these equations, node i is the connected node to DG m. For the candidate DGs, $P^{DG,Ca-Exp}_{m}$ and $Q^{DG,Ca-Exp}_{m}$ are also decision variables.

$$\begin{cases} P^{DG}_{m,k} \leq \alpha_{i,k} \times P^{DG,Ex-Max}_{m} \quad \forall m \in M_{Ex}, \forall k \in K \\ P^{DG}_{m,k} \leq \alpha_{i,k} \times P^{DG,Ca-Exp}_{m} \quad \forall m \in M_{Ca}, \forall k \in K \end{cases} \tag{15}$$

$$\begin{cases} -\alpha_{i,k} \times Q^{DG,Ex-Max}_{m} \leq Q^{DG}_{m,k} \leq \alpha_{i,k} \times Q^{DG,Ex-Max}_{m} \quad \forall m \in M_{Ex}, \forall k \in K \\ -\alpha_{i,k} \times Q^{DG,Ca-Exp}_{m} \leq Q^{DG}_{m,k} \leq \alpha_{i,k} \times Q^{DG,Ca-Exp}_{m} \quad \forall m \in M_{Ca}, \forall k \in K \end{cases} \tag{16}$$

3.2.3 | Power balance

Equations (17) and (18) ensure active and reactive power balance at each node in all modules. Variable $P^{DG}_{m,k}$ and $Q^{DG}_{m,k}$ show the generated active and reactive powers of the connected DG to node i, respectively.

$$\sum_{\forall k \in \mathrm{K}} \left[P^{DG}_{m,k} - P^{L}_{i,k} \right] = \sum_{\ell \in \Lambda_i} flow^{P}_{\ell} \quad \forall i \in N \tag{17}$$

$$\sum_{\forall k \in \mathrm{K}} \left[Q^{DG}_{m,k} - Q^{L}_{i,k} \right] = \sum_{\ell \in \Lambda_i} flow^{Q}_{\ell} \quad \forall i \in N \tag{18}$$

3.2.4 | Line flow limits

Maximum active and reactive flows of the existing and candidate lines are restricted by Equations (19) and (20). It is assumed that each line has a separate limitation for active and reactive powers flowing in them. Therefore, depending on the direction of the flow, the set of possible values for both flows has a shape of $[-flow^{max}, flow^{max}]$. However, the flow will be zero if the line is not operated

which is ensured in these equations by utilizing the binary β_ℓ.

$$-\beta_\ell \times flow_\ell^{P,Max} \le flow_\ell^{P} \le \beta_\ell \times flow_\ell^{P,Max} \quad \forall \ell \in \Lambda \tag{19}$$

$$-\beta_\ell \times flow_\ell^{Q,Max} \le flow_\ell^{Q} \le \beta_\ell \times flow_\ell^{Q,Max} \quad \forall \ell \in \Lambda \tag{20}$$

3.2.5 | Voltage constraints

Equations (21) and (22) are applied for modeling the voltage limits. Also, according to (23) and (24), if DG k is selected as a master unit, voltage magnitude and angle of the corresponding node ($i = \mathrm{N_{DG}}(k)$) will be also set to the controlled value, respectively.

$$\alpha_{i,k} \times 0.95 \le V_{i,k} \le \alpha_{i,k} \times 1.05 \quad \forall i \in N, \forall k \in K \tag{21}$$

$$-\alpha_{i,k} \times \delta^{Max} \le \delta_{i,k} \le \alpha_{i,k} \times \delta^{Max} \quad \forall i \in N, \forall k \in K \tag{22}$$

$$V_{i,k} = \alpha_{i,k} \times V_k^{DG,set} \quad \forall i \in N_{DG} \tag{23}$$

$$-(1-\alpha_{i,k}) \times \delta^{Max} \le \delta_{i,k} \le (1-\alpha_{i,k}) \times \delta^{Max} \quad \forall i \in N_{DG} \tag{24}$$

3.2.6 | Power flow constraints

The introduced method in Reference 50 is used for conducting the load flow calculations. In this reference, an acceptable linear approximation is applied to calculate the bus voltages. The linearized form of power flow equations in distribution networks can be modeled by (25) to (27).

$$\mathrm{F1}_\ell = {r_\ell}/{r_\ell^2 + x_\ell^2} \ , \quad \mathrm{F2}_\ell = {x_\ell}/{r_\ell^2 + x_\ell^2} \tag{25}$$

$$flow_\ell^P = Zflow_\ell^P + \sum_{\forall k \in \mathrm{K}} \left[\left(\delta_{j,k} - \delta_{i,k}\right) \times \mathrm{F2}_\ell + \left(V_{j,k} - V_{i,k}\right) \times \mathrm{F1}_\ell \right] \quad \forall \ell \in \Lambda \tag{26}$$

$$flow_\ell^Q = Zflow_\ell^Q + \sum_{\forall k \in \mathrm{K}} \left[\left(V_{j,k} - V_{i,k}\right) \times \mathrm{F2}_\ell + \left(\delta_{i,k} - \delta_{j,k}\right) \times \mathrm{F1}_\ell \right] \quad \forall \ell \in \Lambda \tag{27}$$

Moreover, Equations (28) and (29) represent the limits of the slack variables, employed to make the equality constraints valid, when two sides of a line are not included in same module. Here, BigM is sufficiently large and is utilized to certify the equality of variables only when binary β_ℓ takes the value of one, but if this binary variable takes on its opposite value, it leaves the variable defined in these two equations open.

$$-(1-\beta_\ell) \times \mathrm{BigM} \le Zflow_\ell^P \le (1-\beta_\ell) \times \mathrm{BigM} \quad \forall \ell \in \Lambda \tag{28}$$

$$-(1-\beta_\ell) \times \mathrm{BigM} \le Zflow_\ell^Q \le (1-\beta_\ell) \times \mathrm{BigM} \quad \forall \ell \in \Lambda \tag{29}$$

3.3 | Budget constraints

The development of load control capabilities in the candidate buses is considered by Equations (30) to (32). Equations (30) and (31) state that the maximum curtailment option in candidate points is realized through the employment of different levels. The total amount of implementable curtailment capacity in each candidate point is also limited by Equation (32).

$$\sum_{k \in \mathrm{K}} P_{i,k}^{LC,Im} = \sum_{s=1}^{Num_{SL}} \left(\sigma_{i,s}^{L} \times St_{i,s}^{L}\right) \quad \forall i \in \overline{N} \tag{30}$$

$$\sum_{s=1}^{Num_{SL}} \sigma_{i,s}^{L} \le 1 \quad \forall i \in \overline{N} \tag{31}$$

$$\sum_{k \in \mathrm{K}} P_{i,k}^{LC,Im} \le MaxLC_i \times \mathrm{P}_i^{Load} \quad \forall i \in \overline{N} \tag{32}$$

Equations (33) to (35) are utilized to model the expansion of DG capacities in candidate locations. The binary variable $\sigma_{m,s}^{DG}$ indicates which candidate capacity ($St_{m,s}^{DG}$) is selected.

$$P_m^{DG,Ca-Exp} = \sum_{s=1}^{Num_{SG}} \sigma_{m,s}^{DG} \times St_{m,s}^{DG} \quad \forall m \in M_{Ca} \tag{33}$$

$$Q_m^{DG,Ca-Exp} = f_m \times P_m^{DG,Ca-Exp} \quad \forall m \in M_{Ca} \tag{34}$$

$$\sum_{s=1}^{Num_{SG}} \sigma_{m,s}^{DG} \le 1 \quad \forall m \in M_{Ca} \tag{35}$$

Equation (36) restricts the installation of sectionalizer at lines with no switching option. Moreover, the installation of candidate tie lines is controlled by Equation (37).

Equation (38) states that the close or open state for a candidate tie line is dependent on its expansion status.

$$\sum_{\ell=1}^{\Lambda^{NS}} Sec_{\ell} \le Num_{sec}^{Max} \tag{36}$$

$$\sum_{\ell=1}^{\Lambda^{Ca}} Inst_{\ell} \le Num_{tLine}^{Max} \tag{37}$$

$$\beta_{\ell} \le Inst_{\ell} \quad \forall \ell \in \Lambda^{Ca} \tag{38}$$

Equation (39) integrates a budget constraint in the optimization problem. This function includes the implementation cost of load curtailments, the expansion cost of generation capacities, and the cost of switching placement (tie lines and sectionalizers), respectively.

$$\begin{aligned} &\sum_{i=1}^{\overline{N}} \sum_{s=1}^{Num_{SL}} \left(\sigma_{i,s}^{L} \times St_{i,s}^{L} \times Cost_{i}^{LC}\right) \\ &+ \sum_{m=1}^{M_{Ca}} \sum_{s=1}^{Num_{SG}} \left(\sigma_{m,s}^{DG} \times St_{m,s}^{DG} \times Cost_{m}^{Gen}\right) \\ &+ \sum_{\ell=1}^{\Lambda^{Ca}} \left(Cost_{\ell}^{Tie} \times Inst_{\ell}\right) \\ &+ \sum_{\ell=1}^{\Lambda^{NS}} \left(Cost_{\ell}^{Sec} \times Sec_{\ell}\right) \le Budget \end{aligned} \tag{39}$$

3.4 | Objective function

Forming the optimal arrangement of efficient modules is the main objective of the allocation problem to achieve the desired modularity. To maximize the efficiency of the arrangement, the number of the involved load points (as a dependency indicator) are also considered besides the involved consumptions in each module. This purpose can be formulated as Equation (40). This function seeks the modules with the highest independency feature and maximum load provision, considering load priorities. Therefore, by taking into account the priority factor of each load point i, the following objective function is proposed:

$$Maximizing: obj = \sum_{k\in K} \left[\left(1 - \frac{\sum_{z\in N} \alpha_{z,k}}{N}\right) \times \left(\sum_{i\in N} \mathrm{Pr}_{i}^{L} \times P_{i,k}^{L}\right) \right] \tag{40}$$

According to Equation (12), the objective function can be rewritten as Equation (41). The second and third term of this function are of nonlinear terms.

$$\begin{aligned} obj &= \sum_{k\in K} \left[\sum_{i\in N} \mathrm{Pr}_{i}^{L} \times P_{i,k}^{L} \right] \\ &\quad - \frac{1}{N} \sum_{k\in K} \left[\left(\sum_{z\in N} \alpha_{z,k} \right) \times \left(\sum_{i\in N} \mathrm{Pr}_{i}^{L} \times \left(\alpha_{i,k} \times \mathrm{P}_{i}^{Load} - P_{i,k}^{LC,Im} \right) \right) \right] \\ &= \sum_{k\in K} \left[\sum_{i\in N} \mathrm{Pr}_{i}^{L} \times P_{i,k}^{L} \right] \\ &\quad - \frac{1}{N} \sum_{k\in K} \left[\left(\sum_{z\in N} \alpha_{z,k} \right) \times \left(\sum_{i\in N} \left(\alpha_{i,k} \times \mathrm{Pr}_{i}^{L} \times \mathrm{P}_{i}^{Load} \right) \right) \right] \\ &\quad + \frac{1}{N} \sum_{k\in K} \left[\left(\sum_{z\in N} \alpha_{z,k} \right) \times \left(\sum_{i\in N} \left(\mathrm{Pr}_{i}^{L} \times P_{i,k}^{LC,Im} \right) \right) \right] \end{aligned} \tag{41}$$

The second term is the multiplication of two sets of binary variables ($\alpha_{z,k}$ and $\alpha_{i,k}$) that each term can be linearized by introducing the auxiliary binary variables $\lambda_{z,i,k}$ and set of linear constraints as equations in (42).

$$\lambda_{z,i,k} = \alpha_{i,k} \times \alpha_{z,k} \xrightarrow{linearizition} \begin{cases} \lambda_{z,i,k} \le \alpha_{i,k} \\ \lambda_{z,i,k} \le \alpha_{z,k} \\ \lambda_{z,i,k} \ge \alpha_{i,k} + \alpha_{z,k} - 1 \end{cases} \tag{42}$$

The third term in Equation (41) is also the multiplication of two sets of binary and continues variables ($\alpha_{z,k}$ and $P_{i,k}^{LC,Im}$). By utilizing auxiliary continues variables $\gamma_{z,i,k}$ and presenting a set of linear constraints in (43), each term of this multiplication can be linearized too. Since we are looking for maximization of $\gamma_{z,i,k}$ variables, then the proposed linearization form in (43) will be valid.

$$\gamma_{z,i,k} = \alpha_{z,k} \times P_{i,k}^{LC,Im} \xrightarrow{linearization} \begin{cases} \gamma_{z,i,k} \le \alpha_{z,k} \times \mathrm{P}_{i}^{Load} \\ \gamma_{z,i,k} \le P_{i,k}^{LC,Im} \end{cases} \tag{43}$$

Besides, the system resiliency index can be defined as Equation (44) and is the ratio of the total number of the formed efficient modules with the highest independency feature and maximum load provision to total consumptions of system active loads. The denominator of this fraction states that for achieving maximum resiliency in the network, each load point should be included in a separate independent module.

$$\mathfrak{R} = \frac{obj}{\sum_{i\in N} \left[\left(1 - \frac{1}{N}\right) \times \left(\mathrm{P}_{i}^{\mathrm{Load}}\right) \right]} \tag{44}$$

4 | NUMERICAL STUDY

Motivated by finding the capability of modularity in the resiliency improvement, this section aims to thoroughly investigate the merits of the proposed framework via two test networks, three case studies, and four different strategies. The two networks are well-utilized in the literature. The first is the IEEE 37 buses network, which is simpler and is used to demonstrate the basic procedure of how the proposed method can be applied to a distribution grid. On the other hand, the second network is the IEEE 84 buses, which presents more complicated networks in practice. The four strategies are representing four different possible approaches. We compare the proposed method (fourth strategy) with other existing methods in different conditions with an analysis of the performance of these strategies. Some parameters in the optimization process directly influence the acquired results. Based on this, we further investigate the impact of different conditions and parameters through three separate cases; namely, we explore the impact of different budget levels, switching capability and load control, and maximum achievable resiliency in case I, II, and III, respectively.

The proposed methodology is programmed in MATLAB environment, and IBM ILOG CPLEX 12.7 software[51] is used to solve the MILP formulation on a personal computer with Intel Core i7 CPU @4 GHz and 16 GB RAM. In all simulations, MIP gap is assumed to be 0.001%.

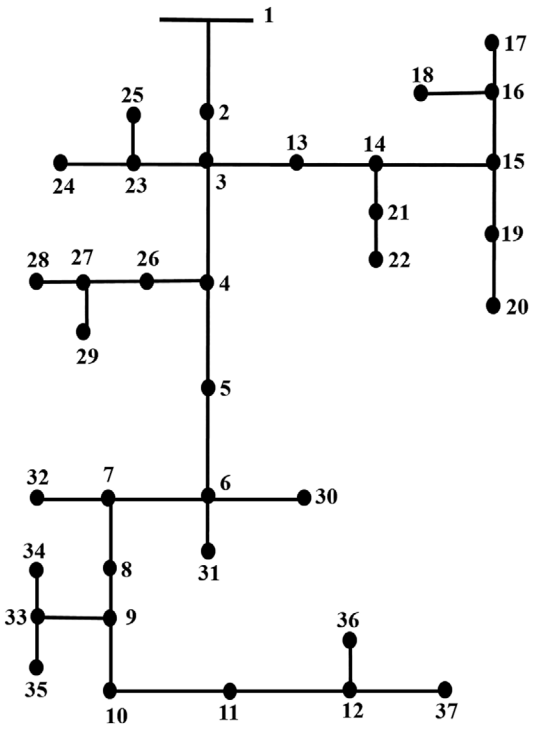

FIGURE 3 Test network I

4.1 | Test network I

In this section for comparing the principle of the proposed investment model with the introduced methods in References 31, 32 modified IEEE 37-bus test network is considered for simulation. The total real and reactive power loads are 981.91 kW and 545.01 kVar, respectively. The line parameters and load consumptions data are given in Reference 52. In this case, disregarding the costs, only allocation of 400 kW generation capacity (in steps of 5 kW) over eight candidate locations (nodes 4, 5, 6, 12, 13, 16, 28, 29) is considered. Maximum installable capacity in each candidate point is also restricted to 200 kW. Single line diagram of this test network is depicted in Figure 3.

Table 2 represents the obtained optimal plans for different strategies. In first, with three strategies (*ST1*, *ST2*, and *ST3*), the problem is solved using the worst-case approach by implementing the defender-attacker model proposed in References 31, 32 for the worst single, double, and triple contingencies, respectively. In addition, in *ST4* strategy, DG allocation is performed based on the modularity idea. In other words, we had the simulation for three different existing approaches and then compared them with the one that is proposed in this study, incorporating the modularity concept into the whole model and optimization framework. According to the results, the number of locations of DGs for the first two strategies is only two; the sizing are the same for these approaches; however, the DGs are located on different buses. This increases for the third strategy, in which four locations are considered for DGs placements, namely: buses 4, 6, 12, and 16. Nevertheless, in ST4, the

TABLE 2 Obtained plans for different strategies

ST1: Based on worst single contingency	ST2: Based on worst double contingency	ST3: Based on worst triple contingency	ST4: Based on modularity concept	
200 kW at bus 16	200 kW at bus 13	180 kW at bus 4	100 kW at bus 12	45 kW at bus 29
200 kW at bus 5	200 kW at bus 6	110 kW at bus 6	90 kW at bus 6	40 kW at bus 13
		60 kW at bus 12	85 kW at bus 4	40 kW at bus 28
		50 kW at bus 16		

modularity approach by choosing six locations for DG installation tries to scatter the generation capacities along with the network leading to a higher modularized structure compared to the other strategies that employ worst-case principles. The presented output for *ST4* in Table 2 includes buses number 29, 13, and 28 in addition to 4, 6, and 12. This issue results in a more resilient plan with higher recoverability in the case of severe events.

Figure 4 compares self-healing capabilities of the obtained plans in case of worst interruptions. In other words, the level of recoverability of each plan for the worst simultaneous k interruptions of the lines is calculated. These worst conditions are not the same for each plan. For example, in *ST1* plan, simultaneous interruptions of the lines *L1* (between nodes 1 and 2) and *L15* (between nodes 15 and 16) are the worst double contingency, but for the *ST2* plan, interruptions of the lines *L1* (between nodes 1 and 2) and *L12* (between nodes 3 and 13) is construed as the worst double contingency.

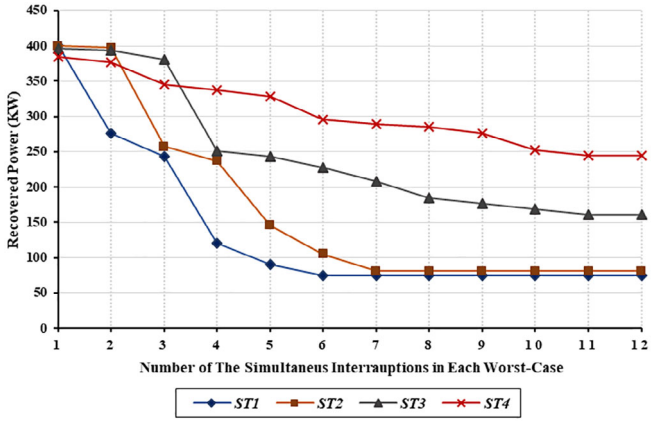

FIGURE 4 The performance of each strategy in case of worst contingencies [Colour figure can be viewed at wileyonlinelibrary.com]

It can be inferred from the results that investing based on the worst-case principle increases the system withstanding for that particular situation but leads to the more fragile structure against the higher intensities. For example, obtained schemes based on the worst double and triple contingencies (*ST2* and *ST3*) have the highest recoverability in corresponding cases, respectively. However, the mentioned schemes are more vulnerable to the severe conditions ($k > 3$) compared to the modularity-based plan (*ST4*). These results emphasize that increasing the penetration of small-scale generations in distribution networks can be very pleasing from resiliency perspectives.

4.2 | Test network II

An 11.4 kV modified 84-bus test system is utilized to investigate the efficiency of the presented model. As shown in Figure 5, this network contains 11 feeders, 84 buses, and 18 sectionalizers. The total real and reactive power loads are 28.350 MW and 20.70 MVar,

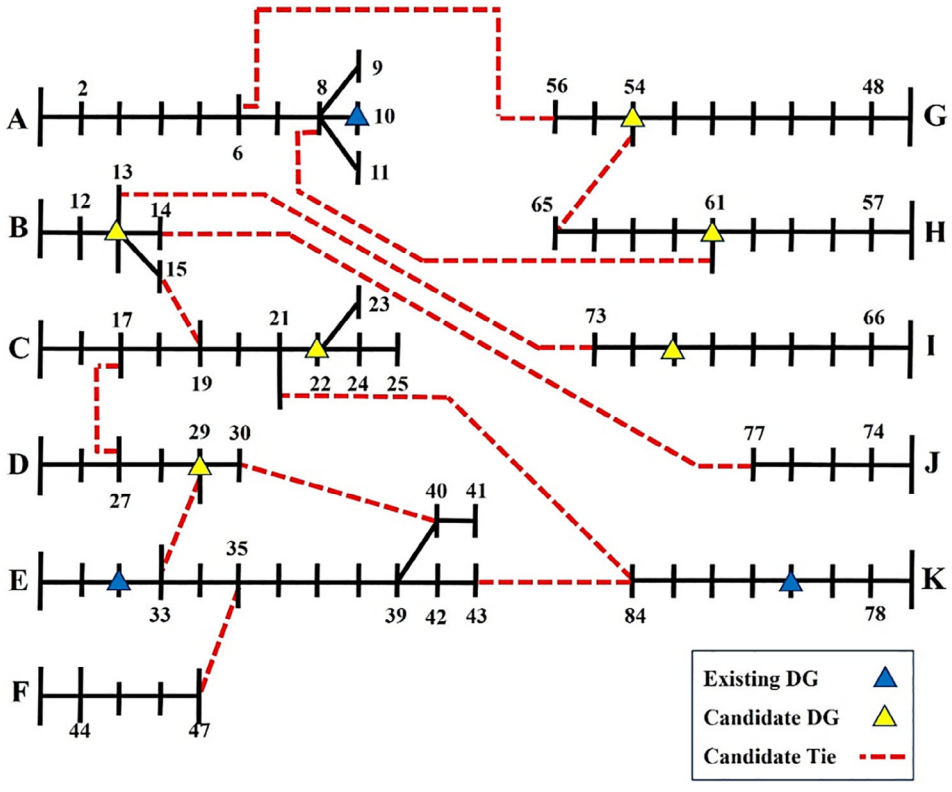

FIGURE 5 Single line diagram of test network II [Colour figure can be viewed at wileyonlinelibrary.com]

TABLE 3 Obtained plans for resiliency enhancement

Budget ($n \times 10^5$ \$)	Lines to install sectionalizers	Selected tie lines	Selected DG capacities	Selected load control options
n = 1	4, 28, 31, 33	Tie1:6-56 Tie8:29-33	0	100 kW at bus 6 100 kW at bus 11
n = 2	4, 28, 35	Tie1:6-56 Tie8:29-33	1000 kW at bus 29	50 kW at bus 7 150 kW at bus 10
n = 3	28, 35	Tie2:8-61 Tie8:29-33	1000 kW at bus 29 1000 kW at bus 54	50 kW at bus 3 50 kW at bus 4 150 kW at bus 9 250 kW at bus 55
n = 4	3, 21, 28, 31, 35	Tie1:6-56 Tie7:21-84 Tie8:29-33	1000 kW at bus 29 500 kW at bus 54 1000 kW at bus 61	0
n = 5	4, 28, 31, 35, 78	84, 91	2500 kW at bus 13 1000 kW at bus 29	200 kW at bus 8 300 kW at bus 14 250 kW at bus 15
n = 6	2, 4, 13, 19, 22, 23, 28, 35, 79	Tie1:6-56 Tie7:21-84 Tie8:29-33	2000 kW at bus 13 1000 kW at bus 22 1000 kW at bus 29	50 kW at bus 6 150 kW at bus 13 100 kW at bus 21 50 kW at bus 55 100 kW at bus 56
n = 7	3, 21, 28, 31, 35, 52	Tie1:6-56 Tie7:21-84 Tie8:29-33	2500 kW at bus 13 1000 kW at bus 29 1500 kW at bus 54	300 kW at bus 14 250 kW at bus 15 200 kW at bus 54 150 kW at bus 65
n = 8	4, 19, 23, 28, 35	Tie1:6-56 Tie7:21-84 Tie8:29-33	2500 kW at bus 13 1500 kW at bus 22 1000 kW at bus 29 1000 kW at bus 61	100 kW at bus 6 300 kW at bus 14 250 kW at bus 15 50 kW at bus 21 50 kW at bus 55 50 kW at bus 56
n = 9	3, 13, 19, 22, 23, 28, 31, 35, 52, 54, 78	Tie1:6-56 Tie7:21-84 Tie8:29-33	2000 kW at bus 13 1500 kW at bus 22 1000 kW at bus 29 1000 kW at bus 54 1000 kW at bus 61	150 kW at bus 13 100 kW at bus 54
n = 10	3, 13, 19, 22, 23, 28, 35, 51, 54, 78	Tie1:6-56 Tie7:21-84 Tie8:29-33	2000 kW at bus 13 1500 kW at bus 22 1000 kW at bus 29 2000 kW at bus 54 1000 kW at bus 61	150 kW at bus 13 100 kW at bus 54

respectively. Information about the load consumptions, line parameters, and switch locations are given in.[53]

In this system, three DG units with a maximum active power capacity of 4 MW are already connected to buses 10, 32, and 80. Maximum reactive power capacity for these existing DGs is set to 4 MVar. As shown in Figure 5, it is assumed that there are six candidate locations for installation of DG units and 12 candidate tie lines. Besides, six discrete sizes from zero to 2.5 MW in steps of 0.5 MW are considered as the candidate capacities. Parameter f_m for the candidate DGs is also set to 0.6. The investment cost for generation expansion is 110 \$/kW. Seven capacities from zero to 300 kW in steps of 50 kW with the investment cost of 20 \$/kW are also considered for creating load curtailment options at all buses. However, the implementation of load control capacity is limited to 50% of the consumption in each load point. Also, the maximum number for installing sectionalizers and tie lines are restricted to 20 and 7, respectively. The installation cost of these elements are assumed to be 9500 \$ and 25 000 \$, respectively. The priority of the loads is also set to one.

4.2.1 | Case I

Table 3 represents the obtained optimal strategy for different budget levels. Based on the results, by increasing the budget, the proposed algorithm appropriately upgrades switching capability, load management options, and generation capacities to enhance the modularity level of the test system. For the first budget level (n = 1), the proposed model has increased the system resiliency about 5% (from 33.08% to 38%) just by applying load curtailments and proper switching. This result indicates the prominence of these flexibilities in the resiliency improvement process. The number of the formed modules, involved loads, objective function, and the system resiliency for each budget level are articulated in Table 4.

Besides, according to Tables 3 and 4, by escalating the budget, the number of the selected DGs for capacity expansion and, correspondingly, the number of the formed modules are also increased. The reason is that the proposed model is more willing to distribute the generation capacities along the network to create efficient modules and benefits higher independency feature. Moreover, based on the results, for every 100 000 $ increase in budget, the resiliency of this system has improved about 2.5%. It can be inferred that resiliency enhancement can be so expensive.

In Figure 6, covering areas of the formed modules for budget level 10 are depicted. In one of these modules, which includes load points 12, 13, and 15, total active and reactive power consumptions are 1800 kW and 1300 kVar, respectively. Since the maximum active and reactive power capacity of the installed DG at bus 13 are 2000 kW and 1200 kVar, for achieving reactive power balance in that module, a load curtailment option is allocated at bus 13. A similar explanation can be presented to validate the considered curtailment at bus 54.

Besides, as it can be seen, none of the connected loads to feeders *I*, *J*, and *F* are involved in these formed modules. It is because the mentioned feeders have generally lower consumptions compared to the others, and fewer numbers of candidate tie lines are connected to them. Consequently, if a module is formed in these feeders, it will suffer from poorer efficiency level. Therefore, according to Figure 7, mostly the feeders with higher power consumptions are selected for modularity enhancement.

Also, in this test network, there are 19 load points with power higher than 500 kW. These loads include 19.5 MW of the total consumptions of the test system. Considering budget level 10, about 66% of these loads (12.9 MW) are covered with the formed modules. In other words, the proposed algorithm for increasing the efficiency of the modules tries to involve the loads with higher consumptions.

4.2.2 | Case II

The impact of switching capability and load control options in improving system resiliency index, considering different strategies, is depicted in Figure 8. Note that resiliency metric is calculated according to Equation (44). Based on the results, in the first strategy, which only considers DG installation, for budget levels 5 to 10, no improvement is achieved. In other words, after a specific point just by allocating generation capacities, modularity enhancement will not be achievable. This item can be relieved by applying the switching capability in strategy 2, creating curtailment options in strategy 3, or implementing both of them in strategy 4. It can be

TABLE 4 Objective function and system resiliency for each budget level

Budget (n × 10^5 $)	Number of the formed modules	Involved loads (kW)	Objective function (kW)	Resiliency index
n = 0	3	10 500	9377.5	0.3347
n = 1	3	11 600	10 773.5	0.3845
n = 2	3	12 600	11 559.2	0.4126
n = 3	4	13 583	12 284	0.4385
n = 4	4	14 210	13 015.2	0.4646
n = 5	4	14 755	13 746.1	0.4907
n = 6	4	15 750	14 511	0.5180
n = 7	5	16 555	15 240.6	0.54406
n = 8	5	17 495	15 946.7	0.56927
n = 9	6	17 989	16 651.7	0.59443
n = 10	6	18 789	17 362.1	0.61979

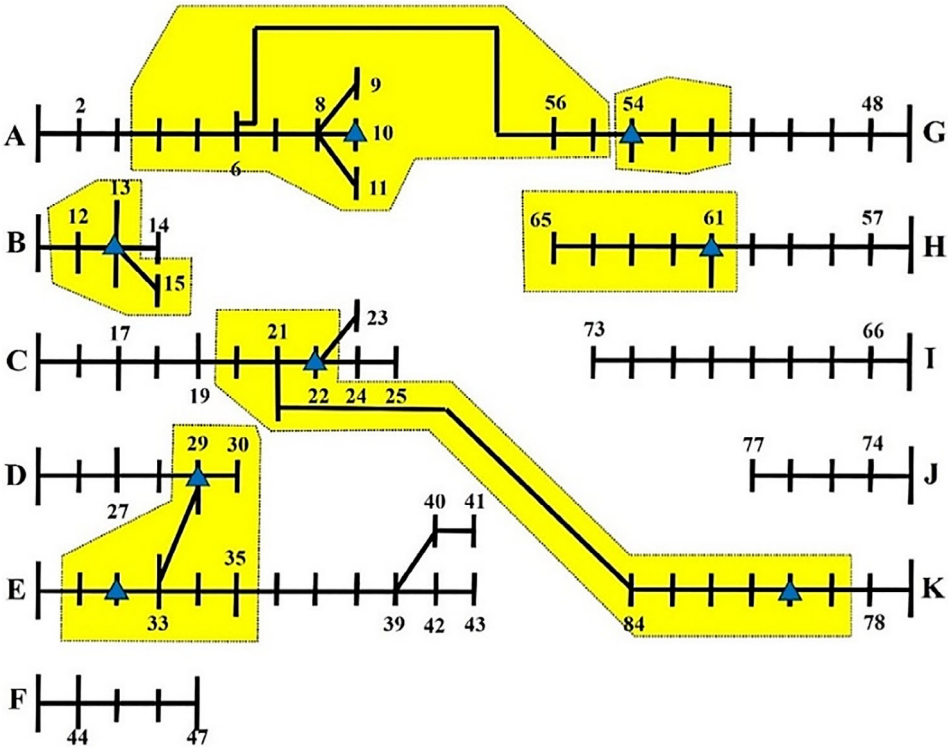

FIGURE 6 Efficient formed modules for budget level 10 [Colour figure can be viewed at wileyonlinelibrary.com]

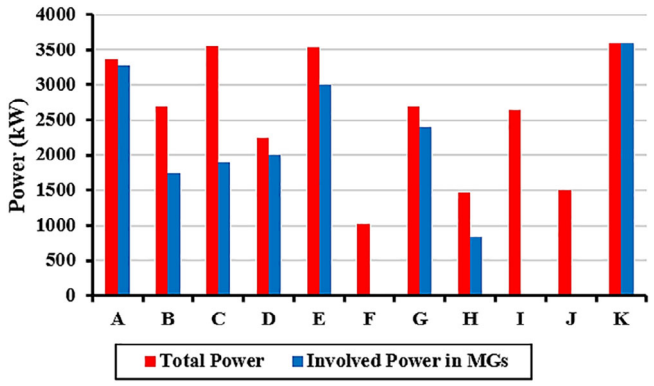

FIGURE 7 Total and involved power in each feeder considering budget level 10 [Colour figure can be viewed at wileyonlinelibrary.com]

concluded that the mentioned flexibilities facilitate the formation of efficient modules in distribution networks, which lead to a higher resiliency.

4.2.3 | Case III

In this section, maximum achievable resiliency without considering budget constraints is discussed. For this purpose, the maximum installable capacity for generation expansion in each candidate location is raised to 3000 kW. Also, the maximum number of the installable sectionalizers and tie lines are increased to 65 and 12, respectively. The obtained optimal investment plan is articulated in Table 5. Moreover, detailed results about the objective function, system resiliency, and the cost are tabulated in Table 6. Covering areas of the formed modules are also depicted in Figure 9.

Based on the results, 19 sectionalizers, 8 tie lines, 18 MW, and 10.8 MVar new generation capacities are added to the test network. Since in this case, there are no shortages in generation capacity compared to the network consumptions; therefore, no curtailments are also needed for modularity enhancement. Implementing this plan costs 2 360 500 $. Besides, 56 load points are involved in the eight formed modules, and they contain 92.34% of the whole network consumptions. Dependency feature of the modules restricts involving of the total consumptions. Moreover, according to Figure 9, *M3* includes two DGs. Since the capacity of the installed DG at bus 22 (3000 kW) is not adequate for providing the set of the connected loads to buses 15, 18, 19, 20, 21, and 22 (3800 kW), the existing DG at bus 80 also participates in forming that module.

According to the results, in this case, which budget restrictive constraints are not applied, the resiliency is just enhanced to 85.4%. Not reaching 100% resiliency is not due to the lack of enough generation capacities; since as shown in Table 5, the total active and reactive capacity of the installed and existing generations in the optimal plan are 30 MW and 22.8 MVar, while the network

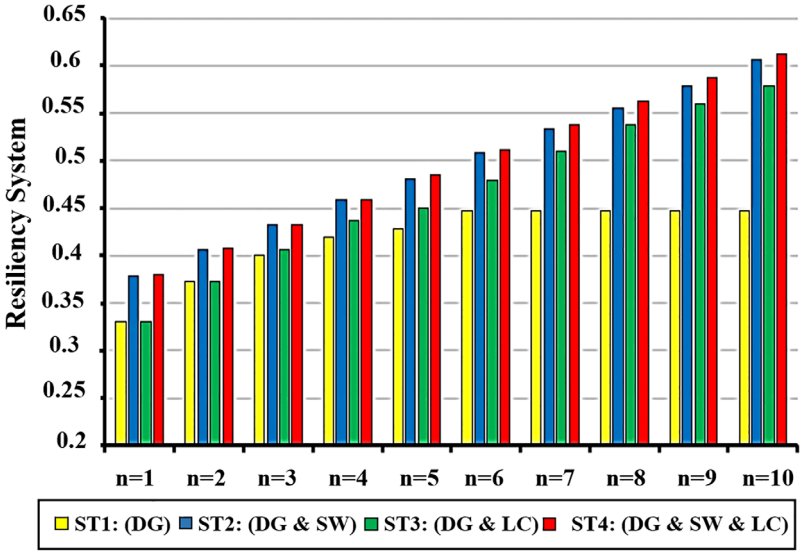

FIGURE 8 Impact of different strategies [Colour figure can be viewed at wileyonlinelibrary.com]

Sectionalizers	Tie lines		DG capacities	Load control
2, 12, 14, 72, 76, 17, 22, 23, 79, 16, 26, 40, 42, 31, 35, 45, 50, 57, 68	Tie3:13-73 Tie4:14-77 Tie5:15-19 Tie6:17-27	Tie7:21-84 Tie8:29-33 Tie9:30-40 Tie10:35-47	3000 kW at bus 13 3000 kW at bus 22 3000 kW at bus 29 3000 kW at bus 54 3000 kW at bus 61 3000 kW at bus 71	0

TABLE 5 Obtained plan considering no budget constraints

TABLE 6 Objective function and system resiliency for each budget level

Cost ($)	Number of the formed modules	Number of the involved load points	Involved loads (kW)	Objective function (kW)	Resiliency index
2 360 500	8	56	26 180	23 925	0.85408

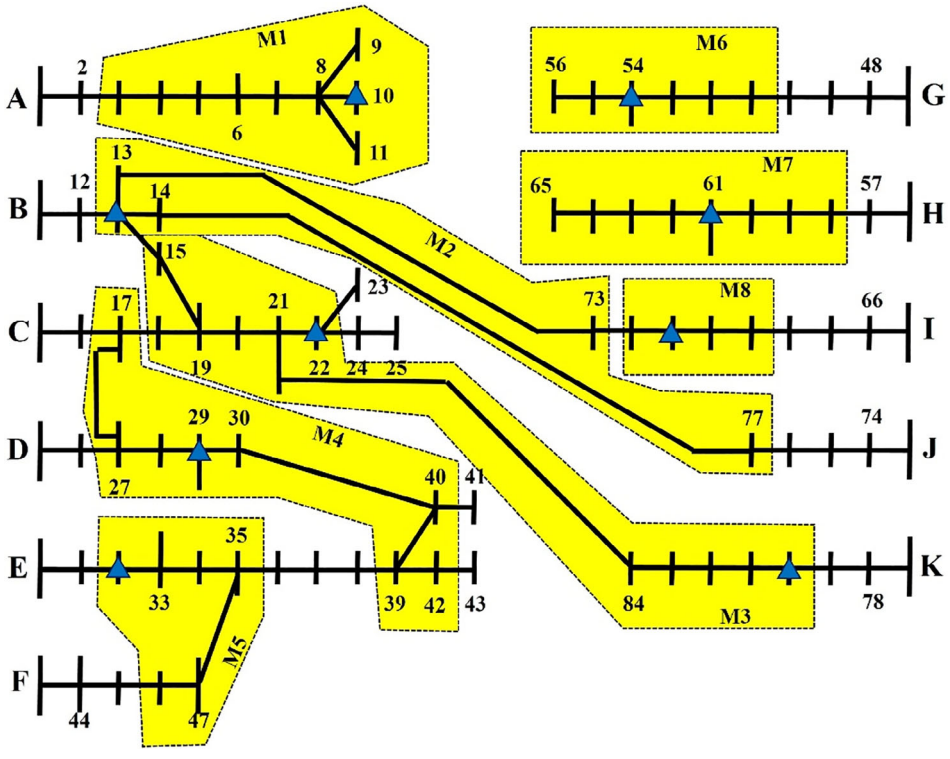

FIGURE 9 Formed modules in case III [Colour figure can be viewed at wileyonlinelibrary.com]

consumptions are 28.35 MW and 20.7 MVar. This level of resiliency is derived because the number of candidate locations for DG installation is limited to six points. In other words, 100% resiliency will be achieved when for every single load in the network, an independent module is formed and its consumption is supplied through the installed DG in that load point.

5 | CONCLUSION

In this paper, a novel resource allocation approach has been presented for resiliency enhancement in distribution networks based on the modularity concept. The proposed model tried to relieve the existing deficiencies in the previous models and focused on resiliency improvement from a new perspective. Some important findings obtained from this paper are highlighted as follow:

- In the proposed resilient resource allocation model, the expansion of DGs capacity, development of switching devices (sectionalizers and tie lines), and the implementation of load curtailment options are all integrated into a mixed-integer linear optimization problem, which leads to the achievement of an effective investment plan in distribution network facilities to enhance the system resiliency.
- Formation of efficient modules has been modeled as the objective function. By applying this method, resiliency improvement performed for different budget levels and various strategies. The results show that the appropriate allocation of the mentioned resources realizes robust energy providing and leads to desired modularity in distribution networks.
- For improving the system performance against the unpredictable severe events, the model considers the independency feature of the formable modules in the expansion process and, for this purpose, distributes the generation capacities along the network to guarantee the efficiency of the modules.
- Since improving the resiliency of networks can be so expensive, implementation of the proposed model will help distribution networks' planners to make better and efficient investment decisions.

In the future works, the resilience-based resource allocation planning scheme can move a step forward in following directions:

- Although the installation of the mentioned facilities brings some other benefits such as loss reduction and economic operations during their lifetime, in this paper, optimal allocation of the budget only from the resiliency perspective is discussed. A multiobjective approach can be proposed for incorporating these items in the future works.
- Development of renewable energies, energy storage systems, line hardening, and determining the optimal emergency budgets for electric utilities can be considered in future research efforts.
- Different type of demand response approaches can be considered in the resource allocation model to improve the resilience of distribution networks.

DATA AVAILABILITY STATEMENT

The data that support the finding of this study are available from the corresponding author upon reasonable request.

NOMENCLATURE

Indices and sets

N	Set of the nodes
$\overline{N}$	Set of the candidate curtailment options
Λ	Set of the lines (candidate and existing)
Λ^{ST}	Set of the switching lines (including tie line)
Λ^{NS}	Set of the lines without switching option
Λ^{Ca}	Set of the candidate tie lines
Ψ_{ℓ}	Set of the nodes belongs to the line ℓ
$\xi_{i,k}$	Set of the parents of the node i to reach the root node k
$Allpath_{a-b}$	Set of the paths between nodes a and b
i	Index of buses
k	Index of modules
K	Set of the formable modules
M	Set of the DGs (candidate and existing)
M_{Ex}	Set of the existing DGs
M_{Ca}	Set of the candidate DGs
N_{DG}	Set of the nodes connected to all DGs
N_{Ca_DG}	Set of the nodes connected to candidate DGs
Λ_i	Set of the connected lines to node i
Λ^a_{b-c}	Set of the lines belongs to the path a between nodes b and c
m	Index of DGs
ℓ	Index of lines

Parameters

Num^{Max}_{Mds}	Maximum number of formable modules
$NumPath_{a-b}$	Number of the paths between nodes a and b
f_m	Indicating reactive capacity factor
$flow^{P,Max}_{\ell} flow^{Q,Max}_{\ell}$	Maximum active and reactive flows of the line ℓ
P_i^{Load}, Q_i^{Load}	Active and reactive power consumptions of the load i

$P_m^{DG,Ex-Max} Q_m^{DG,Ex-Max}$ Maximum active and reactive capacities of the existing DG m

Num_{SG} Number of the candidate capacities steps for generation expansion

Num_{SL} Number of the candidate capacities steps for implementing load curtailment options

$St_{i,s}^{L}$ Candidate capacity for implementing curtailment option at load i and step s

$Cost_i^{LC}$ Cost of implementing one kW curtailment option at load i

$Cost_\ell^{Tie}$ Installation cost of one km tie line ℓ

$Cost_m^{Gen}$ Cost of developing one kW generation capacity in candidate location m

$NumLine_{b-c}^{a}$ Number of the lines in the path Λ_{b-c}^{a}

r_ℓ , x_ℓ The resistance and reactance of line ℓ

$BigM$ A big number

$MaxLC_i$ Maximum curtailments at load i

$St_{m,s}^{DG}$ Candidate expansion capacity for candidate DG m

Num_{sec}^{Max} Maximum number of installable sectionalizers

Num_{tLine}^{Max} Maximum number of installable tie lines

$Cost_\ell^{Sec}$ Installation Cost of sectionalizer at line ℓ

$Budget$ Total budget

Variables

$\alpha_{i,k}$ Binary variable indicating the belonging state of node i to module k

β_ℓ Binary variable indicating the operation mode of the line ℓ

$Zflow_\ell^P$, $Zflow_\ell^Q$ Slack variables

$flow_\ell^P$, $flow_\ell^Q$ Active and reactive power flows of the line ℓ

$P_{i,k}^{LC,Im}$ Implemented curtailment option at load i and module k

$P_{i,k}^{L}$, $Q_{i,k}^{L}$ Provided active and reactive power of the load i in a module k

Pr_i^L Priority factor of the load point i.

$P_{m,k}^{DG}$, $Q_{m,k}^{DG}$ Generated active and reactive powers of DG $m$in module k

$P_m^{DG,Ca-Exp}$, $Q_m^{DG,Ca-Exp}$ Expanded active and reactive capacities for candidate DG m

Sec_ℓ Binary variable indicating the existence of switch on the line ℓ

$\sigma_{m,s}^{DG}$ Binary variable indicating which capacity is selected for DG m

$Path_{b-c}^{a}$ Binary variable indicating the opened or closed mode of the path a

$V_{i,k}$, $\delta_{i,\,k}$ Voltage magnitude and angle of the node i in the module k

$\sigma_{i,s}^{L}$ Binary variable indicating which curtailment capacity is selected at load i

$Inst_\ell$ Binary variable indicating the installation state of the candidate line ℓ

ORCID

Arman Alahyari https://orcid.org/0000-0002-1143-3843
Tohid Ghanizadeh Bolandi https://orcid.org/0000-0002-4284-8742

REFERENCES

1. Esteban M, Portugal-Pereira J, Mclellan BC, et al. 100% renewable energy system in Japan: Smoothening and ancillary services. *Appl Energy*. 2018;224:698-707.
2. Feng W, Jin M, Liu X, et al. A review of microgrid development in the United States—A decade of progress on policies, demonstrations, controls, and software tools. *Appl Energy*. 2018;228:1656-1668.
3. Kahnamouei AS, Bolandi TG, Haghifam MR. The conceptual framework of resilience and its measurement approaches in electrical power systems. *Proceedings of the IET International Conference Resilience Transmission Distribution Network*; Birmingham, UK: IET; 2018:1-11.
4. Zhou W, Krivtchik G, Blaise P. Resilience of nuclear fuel cycle scenarios: Definition, method and application to a fleet with uncertain power decrease. *Int J Energy Res*. 2020;1-22.
5. Moslehi S, Reddy TA. Sustainability of integrated energy systems: A performance-based resilience assessment methodology. *Appl Energy*. 2018;228:487-498.
6. Panteli M, Trakas DN, Mancarella P, Hatziargyriou ND. Power systems resilience assessment: hardening and smart operational enhancement strategies. *Proc IEEE*. 2017;105(7):1202-1213.
7. Schneider KP, Tuffner FK, Elizondo MA, Liu CC, Xu Y, Ton D. Evaluating the feasibility to use microgrids as a resiliency resource. *IEEE Trans Smart Grid*. 2017;8(2):687-696.
8. Mishra DK, Ghadi MJ, Azizivahed A, Li L, Zhang J. A review on resilience studies in active distribution systems. *Renew Sust Energ Rev*. 2021;135:1-20.
9. Rangu SK, Lolla PR, Dhenuvakonda KR, Singh AR. Recent trends in power management strategies for optimal operation of distributed energy resources in microgrids: A comprehensive review. *Int J Energy Res*. 2020;44(13):9889-9911.
10. Tavakoli M, Shokridehaki F, Akorede MF, Marzband M, Vechiu I, Pouresmaeil E. CVaR-based energy management scheme for optimal resilience and operational cost in commercial building microgrids. *Int J Electr Power Energy Syst*. 2018;100:1-9.
11. Zhou Y, Panteli M, Moreno R, Mancarella P. System-level assessment of reliability and resilience provision from microgrids. *Appl Energy*. 2018;230:374-392.

12. Mohagheghi S, Rebennack S. Optimal resilient power grid operation during the course of a progressing wildfire. *Int J Electr Power Energy Syst*. 2015;73:843-852.
13. Lai K, Illindala MS. A distributed energy management strategy for resilient shipboard power system. *Appl Energy*. 2018;228:821-832.
14. Arab A, Khodaei A, Khator SK, Ding K, Emesih VA, Han Z. Stochastic pre-hurricane restoration planning for electric power systems infrastructure. *IEEE Trans Smart Grid*. 2015;6(2):1046-1054.
15. Arab A, Khodaei A, Han Z, Khator SK. Proactive recovery of electric power assets for resiliency enhancement. *IEEE Access*. 2015;3:99-109.
16. Wang C, Hou Y, Qiu F, Lei S, Liu K. Resilience enhancement with sequentially proactive operation strategies. *IEEE Trans Power Syst*. 2017;32(4):2847-2857.
17. Mousavizadeh S, Haghifam MR, Shariatkhah MH. A linear two-stage method for resiliency analysis in distribution systems considering renewable energy and demand response resources. *Appl Energy*. 2018;211:443-460.
18. Hosseinnezhad V, Rafiee M, Ahmadian M, Siano P. Optimal island partitioning of smart distribution systems to improve system restoration under emergency conditions. *Int J Electr Power Energy Syst*. 2018;97:155-164.
19. Qiu F, Li P. An integrated approach for power system restoration planning. *Proc IEEE*. 2017;105(7):1234-1252.
20. Matelli JA, Goebel K. Conceptual design of cogeneration plants under a resilient design perspective: Resilience metrics and case study. *Appl Energy*. 2018;215:736-750.
21. Chen C, Wang J, Ton D. Modernizing distribution system restoration to achieve grid resiliency against extreme weather events: An integrated solution. *Proc IEEE*. 2017;105(7):1267-1288.
22. Wang X, Li Z, Shahidehpour M, Jiang C. Robust line hardening strategies for improving the resilience of distribution systems with variable renewable resources. *IEEE Trans Sustain Energy*. 2018;10(1):386-395.
23. Alsubaie A, Marti J, Alutaibi K, Pietro AD, Tofani A. Resources allocation in disaster response using Ordinal Optimization based approach. *2014 IEEE Canada International Humanitarian Technology Conference, IHTC*; Montreal, QC, Canada: IEEE; 2014:1-5.
24. Figueroa-Candia M, Felder F, Coit D. Resiliency-based optimization of restoration policies for electric power distribution systems. *Electr Power Syst Res*. 2018;161:188-198.
25. Ding T, Wang Z, Jia W, Chen B, Chen C, Shahidehpour M. Multi period distribution system restoration with routing repair crews, mobile electric vehicles, and soft-open-point networked microgrids. *IEEE Trans Smart Grid*. 2020;11(6):4795-4808.
26. Najafi J, Peiravi A, Guerrero JM. Power distribution system improvement planning under hurricanes based on a new resilience index. *Sustain Cities Soc*. 2018;39:592-604.
27. Panteli M, Pickering C, Wilkinson S, Dawson R, Mancarella P. Power system resilience to extreme weather: fragility modeling, probabilistic impact assessment, and adaptation measures. *IEEE Trans Power Syst*. 2017;32(5):3747-3757.
28. Hemmati R, Saboori H, Siano P. Coordinated short-term scheduling and long-term expansion planning in microgrids incorporating renewable energy resources and energy storage systems. *Energy*. 2017;134:699-708.
29. Sekhavatmanesh H, Cherkaoui R. Optimal infrastructure planning of active distribution networks complying with service restoration requirements. *IEEE Trans Smart Grid*. 2017;9(6):6566-6577.
30. Zare-Bahramabadi M, Abbaspour A, Fotuhi-Firuzabad M, Moeini-Aghtaie M. Resilience-based framework for switch placement problem in power distribution systems. *IET Gener Transm Distrib*. 2017;12(5):1223-1230.
31. Lin Y, Bie Z. Tri-level optimal hardening plan for a resilient distribution system considering reconfiguration and DG islanding. *Appl Energy*. 2018;210:1266-1279.
32. Yuan W, Wang J, Qiu F, Chen C, Kang C, Zeng B. Robust optimization-based resilient distribution network planning against natural disasters. *IEEE Trans Smart Grid*. 2016;7(6):2817-2826.
33. Fang Y, Sansavini G. Optimizing power system investments and resilience against attacks. *Reliab Eng Syst Saf*. 2017;159:161-173.
34. Wu L, He C, Dai C, Liu T. Robust network hardening strategy for enhancing resilience of integrated electricity and natural gas distribution systems against natural disasters. *IEEE Trans Power Syst*. 2018;29(5):5787-5798.
35. Zhang H, Ma S, Ding T, Lin Y, Shahidehpour M. Multi-stage multi-zone defender-attacker-defender model for optimal resilience strategy with distribution line hardening and energy storage system deployment. *IEEE Trans Smart Grid*. 2020;12(2):1194-1205.
36. Gao H, Chen Y, Mei S, Huang S, Xu Y. Resilience-oriented pre-hurricane resource allocation in distribution systems considering electric buses. *Proc IEEE*. 2017;105(7):1214-1233.
37. Zhang B, Dehghanian P, Kezunovic M. Optimal allocation of PV generation and battery storage for enhanced resilience. *IEEE Trans Smart Grid*. 2017;10(1):535-545.
38. Sedzro KSA, Lamadrid AJ, Zuluaga LF. Allocation of resources using a microgrid formation approach for resilient electric grids. *IEEE Trans Power Syst*. 2017;33(3):2633-2643.
39. Ding T, Lin Y, Bie Z, Chen C. A resilient microgrid formation strategy for load restoration considering master-slave distributed generators and topology reconfiguration. *Appl Energy*. 2017;199:205-216.
40. Ding T, Liu S, Yuan W, Bie Z, Zeng B. A two-stage robust reactive power optimization considering uncertain wind power integration in active distribution networks. *IEEE Trans Sustain Energy*. 2015;7(1):301-311.
41. Ding T, Li C, Yang Y, Jiang J, Bie Z, Blaabjerg F. A two-stage robust optimization for centralized-optimal dispatch of photovoltaic inverters in active distribution networks. *IEEE Trans Sustain Energy*. 2016;8(2):744-754.
42. Ding T, Yang Q, Yang Y, Li C, Bie Z, Blaabjerg F. A data-driven stochastic reactive power optimization considering uncertainties in active distribution networks and decomposition method. *IEEE Trans Smart Grid*. 2017;9(5):4994-5004.
43. Alahyari A, Ehsan M, Pozo D, Farrokhifar M. Hybrid uncertainty-based offering strategy for virtual power plants. *IET Renew Power Generation*. 2020;14(13):2359-2366.
44. Alahyari A, Pozo D. Electric end-user consumer profit maximization: An online approach. *Int J Electr Power Energy Syst*. 2020;125:106502.
45. Wu X, Wang Z, Ding T, Wang X, Li Z, Li F. Microgrid planning considering the resilience against contingencies. *IET Gener Transm Distrib*. 2019;13(16):3534-3548.

46. Borghei M, Ghassemi M. Optimal planning of microgrids for resilient distribution networks. *Int J Electr Power Energy Syst*. 2021;128:106682.
47. Mousavizadeh S, Bolandi TG, Haghifam MR, Moghimi M, Lu J. Resiliency analysis of electric distribution networks: A new approach based on modularity concept. *Int J Electr Power Energy Syst*. 2020;117:105669.
48. Garber D. *Projection-free Algorithms for Convex Optimization and Online Learning* (PhD dissertation). Technion-Israel Institute of Technology, Faculty of Industrial and Management Engineering; 2016.
49. Fischer J, Heun V. *Theoretical and practical improvements on the RMQ-problem, with applications to LCA and LCE. InAnnual Symposium on Combinatorial Pattern Matching 2006 Jul 5*. Berlin, Heidelberg: Springer; 2006:36-48.
50. Yuan H, Li F, Wei Y, Zhu J. Novel linearized power flow and linearized OPF models for active distribution networks with application in distribution LMP. *IEEE Trans Smart Grid*. 2016;9(1):438-448.
51. ILOG IBM. Cplex 12.7 user's manual, 2017.
52. Distribution test feeders, IEEE Power Energy Society [Online]. http://sites.ieee.org/pes-testfeeders/files/2017/08/feeder37.zip
53. Piccolo A, Siano P. Evaluating the impact of network investment deferral on distributed generation expansion, *IEEE Trans. Power Syst.* 2009;24(3):1559-1567. https://www.dropbox.com/s/yfg5a9eec0qno59/Modified84BusTestSystem-IJEPES.xlsx?dl=0

How to cite this article: Mousavizadeh S, Alahyari A, Bolandi TG, Haghifam M-R, Siano P. A novel resource allocation model based on the modularity concept for resiliency enhancement in electric distribution networks. *Int J Energy Res*. 2021;1–18. https://doi.org/10.1002/er.6676